J Inorg Organomet Polym (2017) 27:201–214
DOI 10.1007/s10904-016-0464-x

Direct Electrochemistry and Catalytic Function on Oxygen Reduction Reaction of Electrodes Based on Two Kinds of Magnetic Nano-particles with Immobilized Laccase Molecules

Yang Yang[1] · Han Zeng[1] · Wen Shan Huo[1] · Yu He Zhang[1]

Received: 16 September 2016 / Accepted: 1 November 2016 / Published online: 7 November 2016

Abstract Synthesized carboxymethylated Chitosan coupled magnetic Fe_3O_4 nano-particles and phthaloyl Chitosan overlapped magnetic Fe_3O_4 nano-particles, were used as enzyme matrices to prepare two prototypes of Laccase-based electrodes. Dependences of structural and operating parameters on characteristics of spectrometry, aggregation status and catalysis for oxygen reduction reaction of surface anchored protein molecules, were investigated and compared by electrochemical means in combination with spectroscopy and transmission electron microscopy. Results from experiments revealed that the latter electrode displayed favorable catalytic effect in oxygen reduction reaction in the absence of mediator. Key factor in limiting the efficiency of catalysis was ascribed to the diffusion process of the substrate into the layer of nano-particles containing Laccase. While the former electrode only showed efficient catalytic effect in oxygen reduction reaction in the presence of electron mediator with rate determining step in mass-transferring of mediator.

Keywords Laccase · Ferriferrous oxide magnetic nano-particles · Carboxymethylated Chitosan · Phthaloyl Chitosan · Direct electrochemistry · Oxygen reduction reaction

✉ Han Zeng
zenghan1289@163.com

[1] Chemistry and Chemical Engineering Academy, XinJiang Normal University, Urumuqi 830054, XinJiang Uyghur Autonomous Region, People's Republic of China

1 Introduction

Enzymatic fuel cell has been the focus of scientific and industrial interest in recent years commonly used enzymes [glucose oxidase (GOx) and Laccase (Lac)] with high efficiency of transformation are available and friendly to environment and living species [1–3]. Investigations [4, 5] indicate the key to improve the performance in energy out-put of enzymatic fuel cell is usually attributed to the procedure of oxygen reduction reaction (ORR) occurred on the biocathode. While the improvement in dynamics of electron transfer between Lac and conductive support should be the crucial step to prepare advanced enzymatic fuel cell in future. Paths to achieve valid electron shuttle between redox proteins and electrodes include two different routes: employment of electron mediator denoted as indirect electron transfer [6–8] and direct electron shuttle in the absence of mediator [9, 10]. To date, the most efficient route to improve the direct electrochemistry of immobilized redox proteins on the electrode as illustrated in [11] can't be applied in the case of Lac molecules because the cofactors of this protein are too sophisticated [12]. Nano-materials after incorporation of bio-molecules are applied in multiple fields such as nanoscale engineering [13], cell growth, sensing and controlling [14], theranostics [15], nano-architectonics and mechnobiology [16] with great importance. It means the application of nano-material or nano-device with incorporated bio-molecules and improvement in their functions would not only lead to better understanding the essence of physiological activities and metabolism of living organism, but also be helpful to utilize complicated forefront technology in an incredible easy way to operate. Based on nano-devices with accommodated bio-molecules, even bio-functions can be modulated by simple hand-like motions in a way of mechanical controlling. Essentially

these applications are all related to bio-electrochemistry between nano-materials and biomolecules (for instance, redox protein discussed in this article is a typical class of bio-molecules and enhanced electro-chemistry between enzymes and nano-devices would facilitate the achievements of goals mentioned previously).

Hybrid nano-composites [17–21] made up of organic component including natural polymer or synthetic polymer (for example: conductive polymer) and inorganic one such as metal or metal oxide nano-particles, magnetic nano-particles, aboriginal minerals and other inorganic compounds has been attracted the interest of investigations because this kind of nano-composite has both superiorities of components which extend their potentiality of application in many fields. It is more important to be realized that this combination of two components in nano-composite may provide new function to promote its applicable value such as in the field of sensor preparation and fabrication of enzymatic fuel cell or other electronic devices. Incorporation of organic component into the inorganic nano-material may improve bio-compatibility of matrix to some bio-molecules without massive loss of conductivity of nano-composite. Magnetic nano-particles are regarded as the promising candidates to accommodate bio-molecules because of facile preparation and separation, controllable dimension and functional group or surface structure of nano-particles, favorable bio-compatibility and conductivity. Existing cases concerning about electrodes modified by magnetic nano-particles with entrapped enzymes [22, 23] show these electrodes have enough room to develop further including simplification of preparation, improvement in mechanical stability and kinetics in electron shuttle. Hitherto few investigations and comparisons concern about the relationship between structure of interface, chemical characteristics of surface-functionalized group for the magnetic nano-particles and the direct electrochemistry and catalytic function of electrodes based on magnetic nano-particles with enzymes [24].

Investigations [25, 26] reveal that nano-devices surface-anchored by aromatic groups containing gigantic π–π conjugation system with enzymes may achieve direct electron transfer in the absence of mediator. However utilization of unstable and toxic chemicals as modifier on the surface of nano-materials restrains their application into extended fields including biomedical practice in vivo. If enzyme carrier may interact with aromatic or hetero-cyclic aromatic compounds with low toxicity through such forms as chemical bonding, physical adsorption and complexation, these could not only attach enzymes firmly on the surface of matrix in the way of site-direction but also probably promote the direct electrochemistry for the π–π stacking effect occurred between binding sites in the vicinity of T_1 site in Lac, shortening the tunnel distance of electron shuttle. Inconductive Chitosan (CTS) and its derivatives which exhibit good bio-compatibility to redox proteins including Lac referred in this article [8] could be linked to or attached on the surface of nano-particles through covalent coupling or hydrogen bonding to secure magnetic nano-particle over-lapped with natural polymer which can easily form thin film with enough strength and suitable conductivity. On the basis of this, two kinds of electrodes based on magnetic nano-particles with incorporated Lac molecules were proposed in this manuscript grounding on routes mentioned above. Direct chemistry and catalytic function in ORR are investigated and compared for both of Lac-based electrodes. Difference of reproducibility, long-term usability, mechanical stability, thermal stability, acid-base endurance and tolerance to enzyme inhibitor: Cl^- of catalytic function on ORR for both electrodes are estimated and analyzed. Dynamics of catalytic cycle for both Lac-based electrodes are parsed and their rate determining steps are confirmed, respectively.

2 Experiment

2.1 Reagents and Apparatus

Lac from *Trametes Versicolor* (M_w: 68000, without any additional purification), 2,6-dimethoxyphenol (DMP), and 2,2′-azinobis-(3-ethylbenzthiazoline-6-sulfonic acid) diammonium (ABTS, purity: 98.5%) are purchased from Sigma reagent Co., Ltd. (USA). *N*-Ethyl-*N*′-(3-dimethylaminopropyl) carbodiimide (EDC) and *N*-hydroxy succinimide (NHS) are secured from Aladin reagent Co., Ltd. (Shanghai, China). Chitosan (CTS, degree of deacetylation: ≥90%, M_w: 250000) is purchased from Shanghai Shengyao Biotech Co., Ltd. (China). Other commercial chemicals are of analytical grade without extra introduction obtained from sinopharm Co., Ltd. (China). Used buffer solution in tests is 0.2 M phosphate buffer solution (PBS) through the adjustment in ratio of citrate vs. potassium dihydrogen phosphate solution. All buffer solutions are prepared with Milli-Q ultrapure water. N_2 and O_2 used in tests are supplied by Nanjing special gas Co, Ltd. (China).

2.2 Materials and Methods

2.2.1 Preparation of Lac-Based Electrodes Grounded on Magnetic Nano-Particles with Surface-Anchored Functional Groups

Magnetic ferriferrous oxide nano-particle, carboxymethylated Chitosan (CMCH) and phthaloyl Chitosan (PHCTS) were synthesized according to the methods illustrated in [27, 28], respectively. Two kinds of Lac-based electrodes were prepared through different procedures as following

subsequently: (a) Lac-based electrode modified by magnetic nano-particles over-lapped with CMCH was prepared through the method mentioned below-firstly 0.5901 g CMCH was added into 60 mL deionized water and 100 mL Fe_3O_4 dispersed phase was poured into this solution agitating at 85 °C for 40 min. Then this mixture was incubated ultrasonically for 40 min and it was transferred to centrifuge tube for sedimentation which lasted for 6 min at the rotating rate of 6000 round min^{-1}, 2K15 type high speed centrifuge obtained from Sigma, Germany. As-prepared black solid phase was re-dispersed into the distilled water and the same centrifugal preparation repeated once more until the supernatant of dispersed phase was at the pH value of 6.0. Black solid phase was collected magnetically after the supernatant was removed from this system. Secured black precipitate was kept at 90 °C overnight to obtain magnetic Fe_3O_4 nano-particle overlapped with CMCH (denoted as Fe_3O_4@CMCH). 50 mg of Fe_3O_4@CMCH was added into the PBS solution (pH = 6.0, EDC and NHS concentrations were 75.0 and 15.0 mM, respectively) containing 0.5 g Lac for magnetically stirring at least 1 h. Mixture was incubated in refrigerator at 4 °C overnight to allow contact adequately. Suspending magnetic nano-particles were separated from the supernatant in the system in the aid of permanent magnet. Obtained nano-particles were rinsed with batches of blank PBS to remove those Lac molecules which were not firmly attached on the surface of matrix. As-prepared magnetic nano-particles with entrapped protein (denoted as Lac/Fe_3O_4@CMCH) were stored in refrigerator at 4 °C before they were applied in the determination. (b) 100 mg PHCTS and 150 mg magnetic Fe_3O_4 were added into 50 mL DMF mechanically stirring for 6 h and suspending nano-particles were separated from the dispersing solvent in the aid of permanent magnet. Collected magnetic nano-particles were kept in oven at the temperature of 80 °C to be dried overnight. Dried nano-particles overlapped with PHCTS were stored for use in future and were denoted as PHCTS-Fe_3O_4. 50 mg of as-prepared magnetic nano-particle (PHCTS-Fe_3O_4) was added into 10 mL of PBS (pH = 4.4) containing 0.5 g Lac and the mixture was incubated at 4 °C magnetically stirring for 8 h. Mixture after sufficient incubation was centrifuged at the rotating speed of 8000 round min^{-1} to isolate nano-particles with entrapped protein molecules from the system. Settlements were rinsed with batches of 0.2 M PBS for two or three times to remove excessive Lac molecules. Magnetic nano-particles with incorporated enzyme molecules (denoted as Lac/PHCTS-Fe_3O_4) were collected in the presence of magnetic field resulting from permanent magnet and were stored in refrigerator at 4 °C for use. Schematic illustration in the procedures of preparation for two kinds of magnetic nano-particles with different overlapping polymers and entrapped Lac was exhibited in Fig. 1.

Combined solutions of rinsing one and supernatant in combination with bulk solution containing Lac were sent for the determination in content of copper ion. Enzyme loading amounts for two kinds of magnetic nano-particles were measured according to the method-graphite furnace atomic adsorption spectrometry (analyst 800 type spectrometer with spectrum ranging from 190 to 870 nm, purchased from Perkin-Elmer company in USA) and equations introduced in [29, 30], respectively. 20 μL fluids of magnetic nano-particles with enzyme molecules and the same volume of those without Lac for both of Fe_3O_4@CMCH and PHCTS-Fe_3O_4 were transferred to pipette and were over-coated on the surface of glassy carbon electrodes (denoted as GCE, diameter: 6 cm, acting as the role of basal support, purchased from Aida Co, Ltd. in Tianjin, China). Electrodes were kept in beaker for drying in ambient temperature to prepare reference electrodes and Lac-based electrodes denoted as Lac/Fe_3O_4@CMCH/GC, Fe_3O_4@CMCH/GC, Lac/PHCTS-Fe_3O_4/GC and PHCTS-Fe_3O_4/GC.

2.2.2 *Characterization for Structure and Morphology of Magnetic Nano-Particles with Entrapped Lac*

Scanning electron microscopy (SEM) was employed to investigate the change in morphology of magnetic nano-particles before and after Lac incorporation with JSM-6700F type field emission scanning electron microscope (Japanese electrical Co, Ltd. JEO). Samples were prepared through dipping of dispersion phase containing magnetic nano-particles with or without Lac onto the support of copper mesh and drying in vacuum subsequently. Structure of magnetic nano-particles were characterized with FT-IR spectra using; BRUKER EQUINDX-55 type infrared spectrometer (from BRUKER Co, Ltd. in Germany). Changes in configuration of active centre in Lac before and after incorporation into matrix were characterized by UV–vis spectroscopy recorded on a U-2810 type spectrophotometer (Shimadzu Company, Japan) at ambient temperature as the following steps: free Lac solution was secured through dissolving Lac into PBS (pH = 6.0) to acquire 5.0×10^{-2} g mL^{-1} bulk solution and was transferred to colorimetric tube for UV–vis determination; 20 μL slurry of nano-particles with or without incorporated Lac for both of Fe_3O_4@CMCH and PHCTS-Fe_3O_4 were dripped onto the surface of ITO panel and dried in air to be prepared for recording UV–vis spectra in colorimeter. Active surface area was estimated with the illustration in [4], i.e.$K_3Fe(CN)_6$ and $K_4Fe(CN)_6$ were used as electrochemical probe and active surface areas for Fe_3O_4@CMCH/GC and PHCTS-Fe_3O_4/GC were calculated to be 0.34 and 0.30 cm^2 which were secured according to the slope of fitting linear plot for electrodes based on magnetic

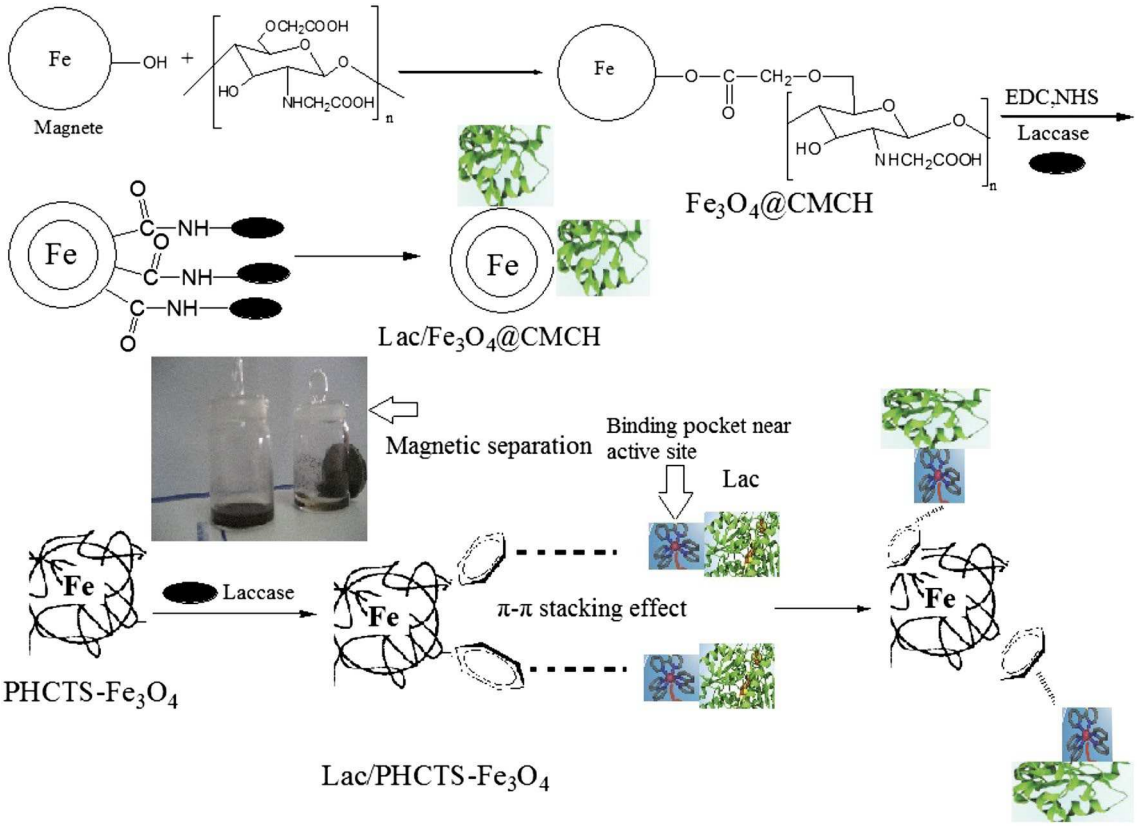

Fig. 1 Schematic illustrations for the immobilization of Lac molecules on the surface of two kinds of functionalized Fe_3O_4 magnetic nano-particles

nano-particles reflecting the dependence of mean value for redox peak current at different potential scanning rate on square root of scanning rate.

Leaching tests for two kinds of nano-particles with Lac were performed as following: 25 mg of magnetic particles were co-mixed with 3 mL PBS (pH = 4.4) stirring for 10 min and were kept in refrigerator at 4 °C for 8 h, respectively. Then the nano-particles with entrapped Lac were extracted from supernatants by using permanent magnet, respectively. Then separated supernatants were mixed with 500 μL 10.0 mM DMP magnetically stirring for 1 min to allow adequate contact and chemical oxidation of DMP, respectively. It followed by monitoring the changes in absorbance at 470 nm with time interval. Absorbance changes were proportional to enzyme leaching amounts originating from magnetic nano-particles in the presence of shearing strength resulting from liquid flowing.

2.2.3 Investigation on Direct Electrochemistry and Catalytic Performance on ORR of Lac-Based Electrode Capped with Magnetic Nano-Particles

Direct chemistry and catalytic effect on ORR for both of Lac-based electrodes over-coated with magnetic nano-particles were investigated with cyclic voltammetry (CV) or linear scanning voltammetry (LSV) together with rotating disk electrode measurement (AFMSRCE rotating disk electrode system from Pine company in USA) recorded on a typical computerized electrochemical working station CHI-1140A (Chen-hua, Shang-hai in China). All electrochemical experiments were performed in a routine three-electrode glass cell connected to electrochemical working station referred previously. PBS in the absence of any external substrate was adopted to be electrolyte in the measurements. Electrodes based on magnetic nano-particles with entrapped Lac were used to be working electrode, with Ag/AgCl (saturated KCl) electrode as the reference electrode and self-made platinum spiral wire as counter electrode. 0.2 M PBS was bubbled with N_2 for at least 30 min ahead of studying direct electrochemical behavior of Lac-based electrode to remove oxygen molecules from the testing system (during the process of measurement, N_2 was introduced into the upper space of the electrolyte to keep the N_2 atmosphere of test), while O_2 was purged into the electrolyte to attain oxygen-saturated PBS when investigating the catalytic effect on ORR (for the same reason, O_2 was piped into the upper of the testing system to maintain the O_2 atmosphere). Catalytic effects on ORR of

enzyme-based electrodes were evaluated by current difference at potential for limited diffusion current $|i_{Oxygen} - i_{Nitrogen}|$. Currents density (j) was derived from normalization of current to active area (As) of electrode (i.e. $j = |i_{Oxygen} - i_{Nitrogen}|/As$). All potentials were relative to normal hydrogen electrode (NHE) without extra statement and all electrochemical experiments were performed at least five times under room temperature (25.0 ± 0.4 °C, except the measurement for the dependence of catalytic function on operating temperature was performed under controllable and variable temperature levels). The change in consistency levels of oxygen dissolved in solution was monitored with Clark type oxygen-detecting electrode was purchased from Hansatech Company of UK.

3 Results and Discussion

3.1 Characterization for Structure and Morphology of Magnetic Nano-Particle with Incorporated Lac

FT-IR spectra of CTS, CMCH, Fe_3O_4, PHCTS and Fe_3O_4@CMCH were shown in Fig. 2. As illustrated in Fig. 2, weak band observed around 2919.1 cm^{-1}, two sharp absorption peaks appeared at 1602.7 and 1423.1 cm^{-1} together with another weak one emerged at 1152.1 cm^{-1} should be ascribed to stretching vibration of methylene, –NH– in imine or –CO– in carboxyl and –C–N– in imine for CMCH, respectively; Fe–O absorption bands at 577.2 and 600.0 cm^{-1} around for magnetic nano-particle Fe_3O_4 were also observed. All absorption peaks in spectra of PHCTS, Fe_3O_4@CMCH and CTS were in accordance with the demonstrations in [27, 28]. It should be emphasized that FT-IR spectrum of Fe_3O_4@CMCH contained characteristic bands for both of CMCH and Fe_3O_4 except new absorption bands at 1150.7 and 1633.3 cm^{-1} attributed to stretching vibrations of C–O–C and C=O were observed. This result indicated surface-tailored –OH groups were successfully linked to carboxyl groups in CMCH, forming the chemical bond of ester (i.e. magnetic nano-particles were overlapped with CMCH in a way of chemical coupling). Furthermore, the chemical bonding process as illustrated in Fig. 1 was confirmed by FTIR spectra of Fe_3O_4@CMCH, free Lac and magnetic nano-particles with chemically tethered Lac which were shown in Fig. 3. It was obvious from comparison between FTIR spectra that most absorbance bands in FTIR spectra of Lac and Lac/Fe_3O_4@CMCH were almost the same except a new absorbance band at 1544 cm^{-1} was observed in FTIR spectrum of Lac/Fe_3O_4@CMCH corresponding to the absorbance peak of δ_{NH} in structure of –CO–NH–. In contrast to FTIR spectrum of Fe_3O_4@CMCH, some absorbance bands which were similar to free Lac were found in FTIR spectrum of Lac/Fe_3O_4@CMCH including absorbance peaks at 1645, 1255, 3417 or 3430 cm^{-1}. These absorbance peaks confirmed the existence of peptide linkage or chemical bonding between –COOH in Fe_3O_4@CMCH and amino group of amino acid residue in Lac. This fact also suggested the chemical structure of immobilized Lac may not be disrupted.

SEM images of morphology for Fe_3O_4@CMCH before and after Lac immobilization were depicted in Fig. 4a, b. Outlines of nano-particles before and after enzyme incorporation were apparently distinct from each other for both of nano-particles with different chemical composition after careful comparison. Morphology of Fe_3O_4@CMCH without immobilized enzyme molecules displayed the formation of gigantic cluster of abnormity (demonstrated in Fig. 4a) resulting from the hydrogen bond interaction between –OH or carboxyl groups in the structural unit of CMCH overlapped on nano-particles which was similar to transmission electron microscopic graph in [27] and SEM image demonstrated in [28]. Although single nano-particle

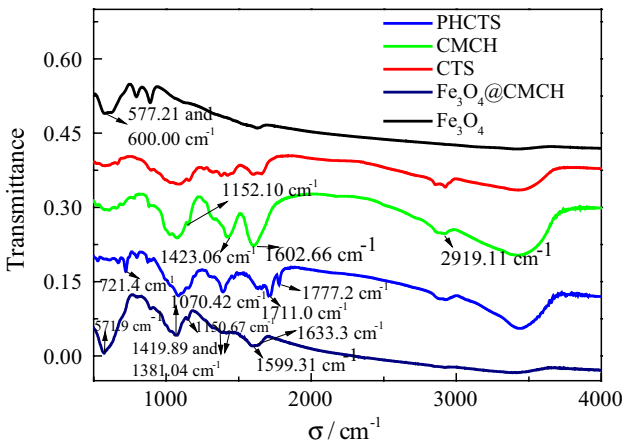

Fig. 2 FTIR spectra of CTS, CMCH, Fe_3O_4, PHCTS and Fe_3O_4@CMCH

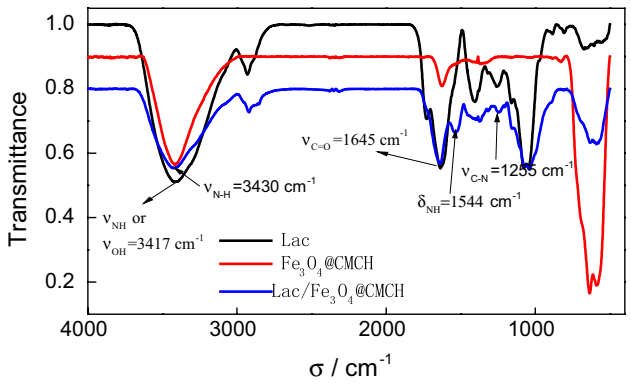

Fig. 3 FTIR spectra of Fe_3O_4@CMCH, free Lac and Lac/Fe_3O_4@CMCH

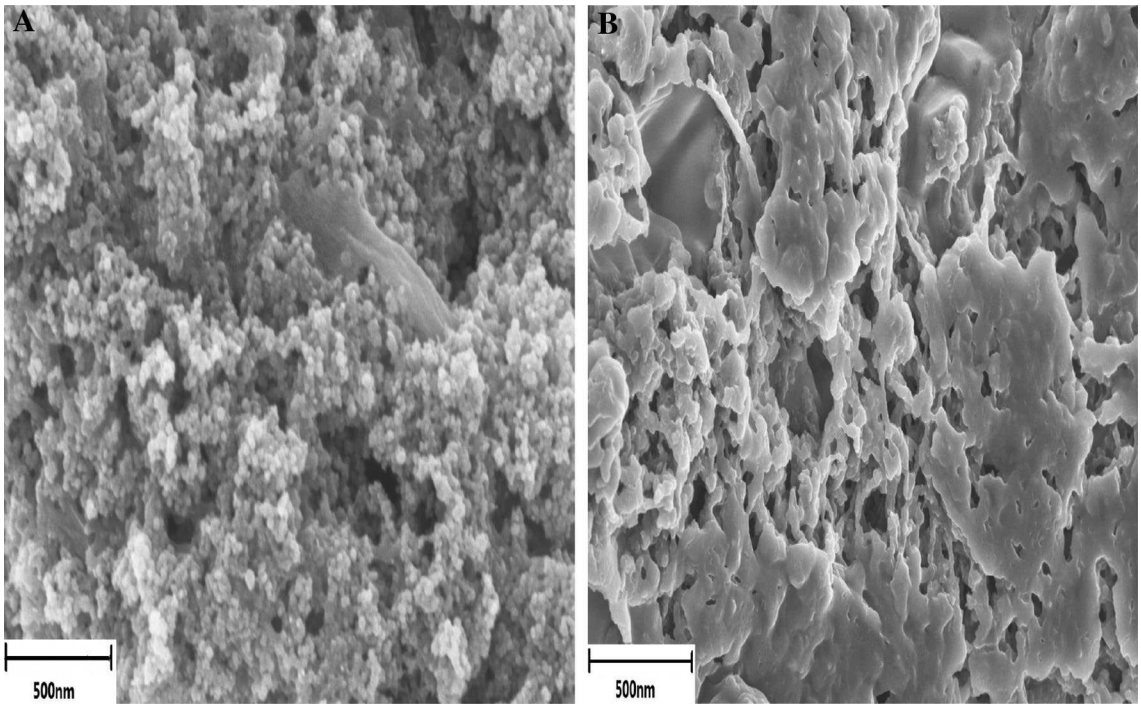

Fig. 4 SEM images of magnetic nano-particles Fe_3O_4@CMCH before (**a**) and after (**b**) Lac immobilization

was hard to recognize, the sheet-like structure resulting from cross-linking of polymer molecules which were not capped on the surface of nano-particles was observed. However the difference between morphologies of nano-particles with different structure should be noticed: in contrast to ordered layer-like array parallel to each other for PHCTS-Fe_3O_4 after Lac incorporation (see Fig. 3b in [28]) originating from site-directed attachment of Lac on the hydrophobic aromatic ring on the surface of PHCTS-Fe_3O_4 via π–π stacking effect between binding site for hydrophobic molecule in Lac as referred in [28], flat plane-like and amorphous layer-assembled structure for Fe_3O_4@CMCH after Lac immobilization rooted in random coupling of surface-anchored carboxyl groups with residue groups such as amino group on the surface of Lac and hydrogen bond interaction between attached Lac molecules which replaced the original appearance of huge cluster of nano-particles aggregation, can be seen in Fig. 4b. The amorphous appearance for Fe_3O_4@CMCH with Lac and partial ordered layer-like arrangement for PHCTS-Fe_3O_4 with entrapped Lac suggested the model of attachment for enzyme incorporation into different matrix differed from variable interaction between functional groups on the surface of enzyme carrier and active site in redox protein molecules.

UV–vis spectra of free Lac and thin film for Fe_3O_4@CMCH with tethered Lac were displayed in Fig. 5. It can be easily seen from Fig. 5 that the same absorption peak at around 605 nm emerged in the scanning scope of

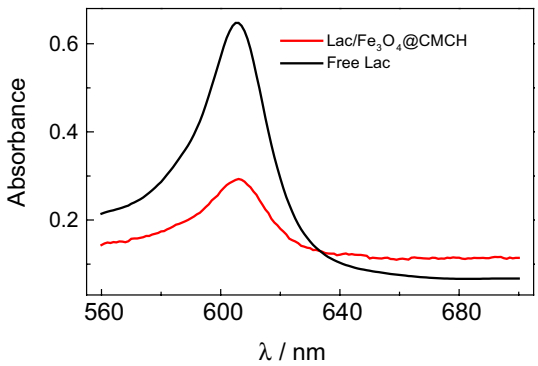

Fig. 5 UV–vis spectra of PBS (pH = 6.0) containing free Lac and thin film of Lac/Fe_3O_4@CMCH

spectra for both of systems mentioned previously which was ascribed to d–d electron transition corresponding to d electron transfer from orbital with lower energy level to that of higher one when fitful residue of peripheral amino acid acted as axial ligands as discussed in [31, 32]. The only difference between them existed in the height of absorption peak resulting from the enzyme loading amount in the carrier (only part of enzyme molecules can be incorporated into the matrix until reaching the saturated loading amount for support.). This result was similar to that depicted in Fig. 2 of [28] and it also revealed the latter displayed higher value of peak height for more enzyme

loading mass in the matrix of PHCTS-Fe_3O_4 (ratio of peak height for Lac/PHCTS-Fe_3O_4 vs. Lac/Fe_3O_4@CMCH was approximately 2:1) which was consonant with the result determined with graphite furnace atomic adsorption spectrometry (enzyme loading amounts for both of them were 210.2 and 102.6 mg g^{-1}, respectively). This result from Fig. 5 also suggested that the interaction between Lac and enzyme carrier didn't interfere with inherent configuration of metal ions in active site of enzyme and their valence state (no extra absorption band corresponding to interaction between central ions in Lac and ligands was observed) which was distinct from that exhibited in Fig. 2B of [31]. This conclusion was in accordance with the analysis on FTIR spectra illustrated in Fig. 3e. meaning the chemical coupling between surface modified –COOH of magnetic nano-particles and amino groups on the surface of Lac molecules didn't influence the inner molecular structure of protein including the inner chemical bonds of Lac, inherent configuration and valence of cofactors in Lac after Lac incorporation into the matrix.

Leaching curves for two kinds of magnetic nano-particles with incorporated Lac which adequately contacted with PBS containing DMP were exhibited in Fig. 6. Results as shown in Fig. 6 manifested that the absorbance change in PBS for Lac/Fe_3O_4@CMCH was slower than that for Lac/PHCTS-Fe_3O_4 within the same time scale (rate of absorbance change for Lac/Fe_3O_4@CMCH was only 5×10^{-5} s^{-1}, being half of that exhibited in [33] and being half of that for Lac/PHCTS-Fe_3O_4), verifying its better mechanical stability than the latter. Advantage in mechanical stability for Lac/Fe_3O_4@CMCH should be attributed to the way of enzyme immobilization with chemical coupling which was reasonably more stable than that for Lac/PHCTS-Fe_3O_4 with physical interaction (π–π stacking effect). Experiment result from graphite furnace atomic adsorption spectrometry which indicated the consistency level of copper ion dissolved in PBS contacted with Lac/PHCTS-Fe_3O_4 was 50%

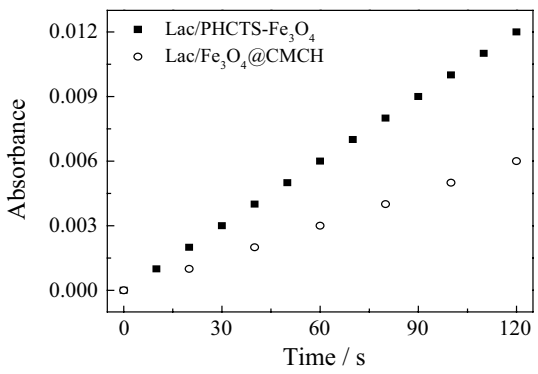

Fig. 6 Enzyme leaching curves for two kinds of magnetic nano-particles with immobilized Lac

higher than that for PBS engaged with Lac/Fe_3O_4@CMCH supported this conclusion.

3.2 Direct Electrochemical Behavior and Catalytic Performance in ORR of Electrodes Based on Magnetic Nano-Particles with Lac Characterized with Electrochemical Means

3.2.1 Direct Electrochemistry and Catalysis for ORR of Lac-Based Electrodes

Two standards were used to judge whether direct electron transfer achieved between conductive support and immobilized redox protein as following: (a) whether apparent electrochemical signals (i.e. redox peaks) attributed to electrochemical transformation of active site in enzyme can be observed in the absence of any substrates and electron mediators; (b) whether catalytic signal (i.e. catalytic wave or current) can be detected in the presence of corresponding substrate. According to these criterions, distinct cases occurred for both of Lac-based electrodes: no apparent redox signal was identified within the range of potential sweeping for both of electrodes: Lac/Fe_3O_4@CMCH/GC, Fe_3O_4@CMCH/GC (see Fig. 7a); similar case occurred for reference electrode: PHCTS-Fe_3O_4/GC (see Fig. 7b), indicating no redox groups contained in enzyme carriers: Fe_3O_4@CMCH and PHCTS-Fe_3O_4. While a pair of redox peaks separated from background currents with mid-wave potential at 798 mV (this value was close to formal potential determined for T_1 site in Lac: 780 mV [28] and potential difference between redox peaks was 114 mV) and ratio of oxidation peak current vs. reduction one ($i_{p,a}/i_{p,c}$) at 1.6 for Lac/PHCTS-Fe_3O_4/GC was observed within the corresponding potential scanning as illustrated in Fig. 4 of [28]. Another fact from experiments should be noted that both of reference electrodes can't catalyzed the oxidation of substrate (DMP and ABTS) and both of working electrodes can do that. These results revealed although both of Lac-based electrode can maintain the inherent configuration and catalytic activity of immobilized enzyme molecules, their direct electrochemistries of entrapped redox protein were completely different originating from distinct interaction between enzyme and matrix. Apparently site-directed adsorption illustrated previously promoted direct electron transfer between them [22, 30]. These also indicated redox signal observed for Lac/PHCTS-Fe_3O_4/GC should be ascribed to electrochemical transformation in active site T_1 of Lac [33]. Further investigation from curves recorded at variable potential sweeping rates for Lac/PHCTS-Fe_3O_4/GC in deaerated PBS and fitting linear plot of anodic peak currents and cathodic ones vs. scan rates (see Fig. 5 in [28]) demonstrated direct electron transfer occurring on the interface of this Lac-based electrode be ascribed

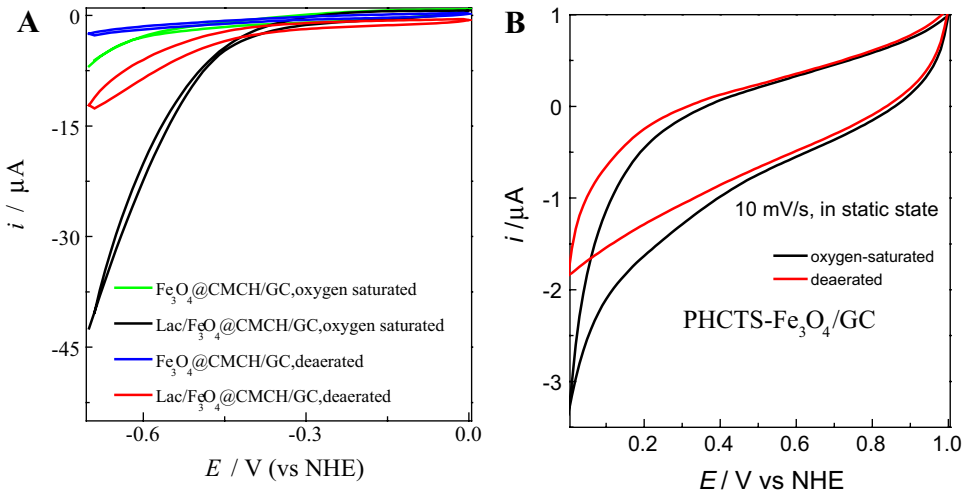

Fig. 7 Catalytic effect on ORR of Lac/Fe_3O_4@CMCH/GC evaluated by CV (**a**) and CVs of PHCTS-Fe_3O_4/GC recorded in deaerated and oxygen-saturated PBS, respectively (**b**). pH of PBS was kept at 4.4, scan rate of potential sweeping was 10 mV s^{-1} for both cases

to a typical surface-confined and quasi-reversible single electron shuttling process (oxidation peaks and reduction ones emerged around 850 and 750 mV, respectively. Peak potentials for anode and cathode didn't shift prominently within the potential sweeping range. $i_{p,a}/i_{p,c}$ ranged from 1.2 to 1.6 and good linear relationship of $i_{p,a}$ and $i_{p,c}$ vs. scan rate retained within the range of sweeping rates. Usually redox process for T_1 site of Lac was regarded to be electro-transformation of one electron transferring as referred in [33]). Electrically wired enzyme coverage on the surface of electrode (Γ) was evaluated through the normalization of mean peak area resulting from integration of redox peaks in CVs recorded at variable scan rates to sweeping rate to be 1.5×10^{9} mol cm^{-2} according to the equation: $\Gamma = Q/ZFA$ (Q is normalization value of average peak area of integration to scan rate which deducts electric charge of double layer charging from the whole value, i.e. Faraday electric charge, Z means electron transfer number in the process of electrochemical transformation, A is surface active area). This value estimated was 325 times of that in the form of densely arrayed with monolayer coverage of Lac illustrated in [33] (4.64×10^{-12} mol cm^{-2}) and higher than that of multi-layer coverage of Lac on nano-porous gold material based electrode (2.1×10^{-11} mol cm^{-2}) demonstrated in [33]. Electrically wired proteins attached on the surface of electrode in the arrangement of specific configuration to form the structure of orientated layers made up of magnetic nano-particles over-lapped with enzymes which achieved direct electron transfer. For this reason, surface coverage of electrically communicated redox protein molecule was apparently higher than that of densely-packed monolayer arrangement estimated theoretically in the former part referred previously.

CVs of Lac/Fe_3O_4@CMCH/GC in deaerated and oxygen-bubbled PBS recorded at the sweeping rate: 10 mV s^{-1} were displayed in Fig. 7a. CVs of reference electrode: PHCTS-Fe_3O_4/GC immersing in deaerated and oxygen-saturated PBS recorded at the same scan rate were shown in Fig. 7b. It can be deduced from Fig. 7a that cathodic reduction current for Lac/Fe_3O_4@CMCH/GC began to increase sharply at −0.40 V in the presence of oxygen, indicating slight catalysis on ORR relative to the case of Fe_3O_4@CMCH/GC (onset potential for ORR was −0.56 V, almost be the same value to that for bare GCE, data not shown). This inferior catalysis on ORR was consistent with indirect electrochemistry of Lac-based electrode, originating from the randomly distributed redox molecules which were chemically coupled to nano-particles through the formation of chemical bond between carboxyl groups on the surface of nano-particles and amino groups on the interface of Lac molecules. Therefore only few immobilized enzyme molecules adopted the proper configuration which facilitated the direct electron transfer to accomplish catalytic function on ORR. This conclusion was in accordance with that analyzed from SEM images in Fig. 4. In contrast to this case, electrically wired Lac for Lac/PHCTS-Fe_3O_4/GC exhibited opposite case in comparison to the former. Reduction peak emerged at 747 mV around for this Lac-based electrode in N_2-bubbled electrolyte and the similar electrochemical signal was observed at 760 mV for this electrode in O_2-saturated PBS (see Fig. 6 in [28]) which was near to the formal potential for T_1 site of Lac [30]. Onset potential of ORR for Lac/PHCTS-Fe_3O_4/GC in oxygen-bubbled PBS when negative sweeping was at around 930 mV, only 40 mV lower than the theoretical formal potential for ORR under the reversible condition and the assumed pH value. It should be noticed that this onset potential for Lac-based electrode mentioned above convinced its superiority in lowering the over-potential of ORR in comparison to that for the reference electrode without Lac as illustrated in Fig. 6b (onset potential for ORR was around 450 mV). Rate constant of direct electron transfer (k_c) for Lac/PHCTS-Fe_3O_4/GC

can be deduced from the secured steady catalytic current density (j) of electrochemical reduction at 500 mV (28.4×10^{-6} A cm^{-2}) in combination with enzyme coverage (Γ) estimated in the saturated status to be 0.05 s^{-1} in the light of equation: $j=nk_c\Gamma F$ (n was assumed to be four in the Lac induced electro-transformation of oxygen into water). It should be emphasized that the efficient catalysis on ORR for Lac/Fe_3O_4@CMCH/GC can be achieved only in the presence of external electron mediator such as ABTS (see Fig. 8). It was obvious from Fig. 8 that a pair of redox peak ($i_{p,a}/i_{p,c}=1.2$, difference between oxidation peak potential and reduction one was 104 mV) corresponding to the transformation between oxidized species and reduced one of ABTS was observed when the electrolyte was nitrogen purged. This redox transformation was classified into a typical electrochemical process limited by diffusion of quasi-reversible one electron transfer as illustrated in [34]. While the electrolyte was purged with O_2, CV for the same electrode recorded at the same scan rate was distinct from that described previously in that the enhanced intensity of reduction peak and the disappearance of the oxidation one, meaning the sigmoidal feature of *i-E* curve. This phenomenon featured the prominent catalysis on ORR for immobilized Lac on the magnetic nano-particles based electrode in the presence of external electron relay. This notable catalytic function resulted from the promotion in electrochemical reduction of enzymatic oxidized species of ABTS into reduced one and the suppression in electro-oxidation for $ABTS^{2-}$.

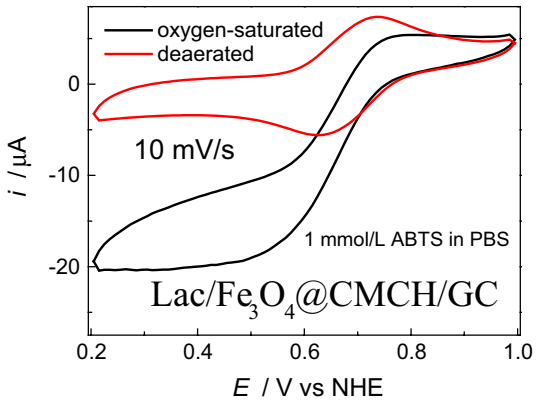

Fig. 8 Catalytic effect on ORR of Lac/Fe_3O_4@CMCH/GC characterized by CV in the presence of electron mediator ABTS (1.0 mM, scan rate: 10 mV s^{-1})

3.2.2 *Reproducibility, Long-Term Usability and Mechanical Stability of Catalysis on ORR for Lac-Based Electrodes*

Comparison in limit catalytic densities of five as-prepared Lac-based electrodes discussed previously with specific procedure of preparation and different chemical composition of magnetic nano-particles working at the same oxygen-bubbled PBS (pH = 4.4, scan rate for both electrodes was 10 mV s^{-1}, ABTS concentration level in the solution was 1 mM for the case of Lac/Fe_3O_4@CMCH/GC and no mediator was present in the electrolyte for the case of Lac/PHCTS-Fe_3O_4/GC) was illustrated in Fig. 9a. Result from Fig. 9a demonstrated that the difference of current density among 5 Lac/PHCTS-Fe_3O_4/GC electrodes could be neglected and that among 5 Lac/Fe_3O_4@CMCH/GC electrodes was apparently distinct although the latter showed higher limited catalytic current for electro-chemical reduction of oxygen than the former in the presence of external mediator. This fact convinced that the former exhibited better reproducibility of catalysis on ORR. Figure 9b illustrated the relationships between catalytic activity on ORR for two kinds of Lac-based electrodes (Lac/PHCTS-Fe_3O_4/GC and Lac/Fe_3O_4@CMCH/GC) operating in the same

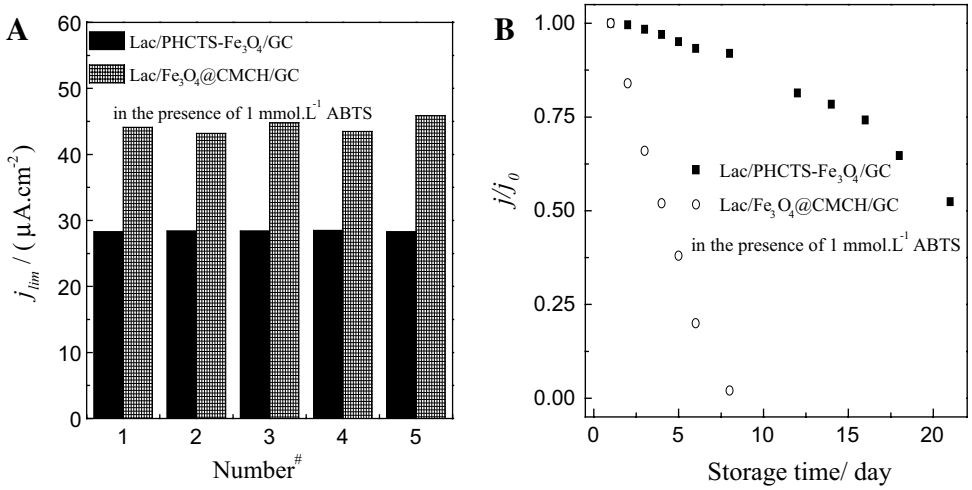

Fig. 9 Reproducibility (**a**) and long-term stability (**b**) of electrodes based on two kinds of magnetic nano-particles with immobilized Lac, test conditions as Fig. 6 of [28] and Fig. 8 demonstrated, respectively. j_0: maximum current density

electrolyte and storage duration of electrodes (scan rate was set at 10 mV s^{-1} for both of electrodes). It was obvious that the former displayed more favorable long-term usability than the latter for lacking of chemical stability in terms of electron mediator in the long run (above 3/4 of initial maximum in catalytic current density for the former can be retained after storage for 14 days, while catalytic activity for the latter was completely lost only after incubation for more than a week). All results mentioned above indicated clearly that Lac/PHCTS-Fe_3O_4/GC which achieved direct electron transfer between enzyme and electrode demonstrated better catalytic function than Lac/Fe_3O_4@CMCH/GC which displayed efficient electron shuttle in the aid of external mediator relay did in whether the reproducibility or the long-term usability. This should be originated from degeneration in chemical stability of mediator with the increase of recycling number or the prolonging of storage duration except for the influence of used chemical reagent to the capability in catalysis on ORR of Lac in immobilized state.

LSVs for both of Lac-based electrodes (Lac/PHCTS-Fe_3O_4/GC and Lac/Fe_3O_4@CMCH/GC) in oxygen-saturated PBS recorded at the same sweeping rate and variable rotating rates of the electrode were shown in Fig. 7 of [28] and Fig. 10, respectively. As demonstrations in Fig. 7 of [28] and Fig. 10 in this article, both electrodes under their operating conditions showed favorable mechanical stability which was different from the case of redox hydrogel depicted in [35]. Catalytic current density in steady state of ORR for Lac-based electrode: Lac/PHCTS-Fe_3O_4/GC can reach 87.7 μA cm^{-2} even at the high rotating rate of electrode: 4000 round min^{-1}. No apparent broken aperture or hollow cave and any sign indicating leakage of immobilized enzyme molecules on the modification layer of electrode surface into the electrolyte was observed providing two side proofs that no notable change in absorbance of the solution at the wavelength of 425 nm corresponding

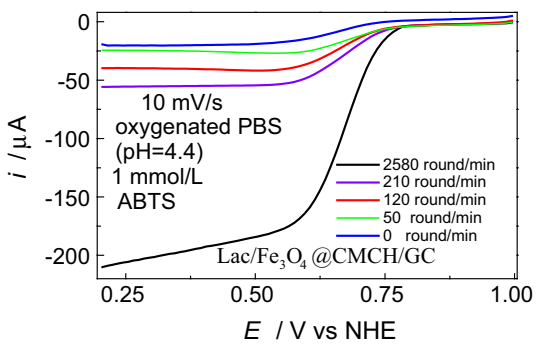

Fig. 10 LSVs of Lac/Fe_3O_4@CMCH/GC in oxygen purged PBS containing 1 mM ABTS recorded under variable electrode disk rotating rates at the scan rate of 10 mV s^{-1}

to maximal absorbance for oxidized species of ABTS was identified after adding 1 mM ABTS into the solution which was isolated from Lac-based electrode and copper ions in the same solution was not detected with graphite furnace atomic adsorption spectrometry. Moreover the fact that the onset potential for ORR, potential of reduction peak or the potential corresponding to the limited catalytic current didn't shift apparently when rotating speed of electrode ranging from 0 to 4000 round min^{-1} indicated improvement in mass transferring (accelerating the process of oxygen penetration into the thin layer made up of magnetic nano-particles with Lac on the surface of electrode) from the elevation in rotation rate of electrode can't influence the catalytic mechanism of Lac-induced ORR but result in the enhancement of limited catalytic current. Turnover frequency of ORR for Lac-based electrode was estimated to be 0.3 s^{-1} and diffusion velocity of oxygen into the layer referred previously on the interface of electrode was determined to be 6.4×10^{-8} cm^2 s^{-1} according to the means depicted in [34], much lower than that measured in solution (1.7×10^{-5} cm^2 s^{-1}) [36]. Acting as the same method illustrated in [34], apparent rate of diffusion for oxidized species of mediator: ABTS (D_{app}) was evaluated to be 4.5×10^{-6} cm^2 s^{-1} from dependence curve of limited diffusion current of cathode vs. rotating rate of electrode demonstrated in Fig. 10. Currents controlled by kinetics at variable over-potentials (i_k) were calculated according to the intercept of double-reciprocal curves reflecting the dependence of Faraday currents at different over-potential in the controlling zone of mass-charge transfer hybrid (i) on square roots of rotating rates (Faraday current derived from the value after background current subtraction and double layer charging current must be adjusted because Faraday current at lower over-potential was close to double layer charging current at slow rotating rate). Then the rate of electro-chemical reduction occurred on the interface of electrode for oxidized species of ABTS under the equilibrium potential (k_0) was figured out to be 5.84×10^{-3} cm s^{-1}. Electro-active zone thickness (Δ) was calculated according to the equation: $\Delta=(D_{app}/k_{cat})^{1/2}$ as the definition introduced in [37] and revision in terms of current system (k_{cat} was steady rate constant of catalysis for ORR determined to be 68.0 s^{-1} according to the method given in [37] when electrolyte was oxygen purged). Standard rate constant (k_s) was derived from the normalization of k_0 to Δ and this calculated value was 23.0 s^{-1}.

3.2.3 Thermal Stability, Acid-Base Endurance and Tolerance to Inhibitor of Catalysis on ORR for Lac-Based Electrodes

Dependence relationship curves of limited catalytic current density on pH of solution and operating temperature

for two Lac-based magnetic nano-particles modified electrodes which were investigated under the same experimental conditions as referred in Fig. 8 were shown in Fig. 9 (Lac/PHCTS-Fe_3O_4/GC) of [28] and Fig. 11 (Lac/Fe_3O_4@CMCH/GC) of this article, respectively. From Fig. 9 in [28] and Fig. 11a in this article, relationships between catalytic activity on ORR for both of electrodes and pH value of electrolyte were similar to that of free Lac as depicted in [29], indicating the existence of optimal pH: pH = 3.0 for free Lac while pH = 6.0 and 4.4 for Lac/Fe_3O_4@CMCH/GC and Lac/PHCTS-Fe_3O_4/GC in oxygen purged PBS, respectively. This may be attributed to partial neutralization of peripheral OH^- near the interface of enzyme carrier with H^+ released by surface-anchored acidic groups in nano-particles with Lac (presence of OH^- would interfere with chemical adsorption of oxygen on active site of Lac) and impact resulting from variable interactions between enzyme carrier and immobilized protein molecule [8]. It can be seen from Fig. 9 in [28] and Fig. 11b of this article that distinct characteristics in dependence of catalytic effect on ORR on operating temperature for two Lac-based electrodes: limited catalytic current density for Lac/Fe_3O_4@CMCH/GC dropped gradually with the elevation of temperature within the testing range of temperatures. When the operating temperature exceeded to 55 °C, catalytic activity in ORR for this electrode decreased drastically. This could be blamed on the deterioration in electron relaying capability of mediator under higher temperature (this factor dominated the degeneration of relaying function for ABTS before 55 °C), desorption of enzyme molecules from the surface of carrier at even higher temperature (color change in solution which contacted with Lac-based electrode would be obvious within one minute if ABTS or DMP was injected into the solution when the temperature-higher than 55 °C. At the same time result from graphite furnace atomic adsorption spectrometry also confirmed the ascension in consistency level of copper ion dissolved in electrolyte was remarkable) and denaturation of redox protein molecules at high temperature. In contrast to this, case of Lac/PHCTS-Fe_3O_4/GC was completely diverse in the bell shape of dependence curve between catalytic effect and temperature within the same testing range. It also meant the so-called transition point at 55 °C could be pinned down through measurement (i.e. before this temperature, catalytic function would rise with the elevation of temperature and would fall with continuous lifting in temperature after that climax). This result was similar to that for Lac-based electrode based on redox hydro-gel demonstrated in [35] and the Lac-based electrode discussed in this article exhibited better mechanical stability in comparison to that illustrated in [35]. Apparent active energy of catalysis on ORR for this Lac-based electrode and apparent active energy of enzymatic denaturation were estimated to be 38.2 and 58.8 kJ mol^{-1} according to the dependence curve of limited catalytic current density on temperature, respectively. Moreover the relationship between rate in enzymatic oxidation of DMP and operating temperature (rate of enzymatic oxidation of DMP increased with the elevation of temperature before 55 °C and it dropped drastically with continuous ascension of operating temperature after 55 °C similar to that illustrated in Fig. 11b) also provided a side proof to support the conclusion that the immobilization of Lac in the matrix of Fe_3O_4@CMCH should be classified into a typical case of chemical adsorption (considered this case has been demonstrated in Fig. 7 of [35], this data was not shown). Denaturation of Lac originating from the distortion in inherent configuration of cofactor in Lac or damage in coupling between carrier and enzyme molecule may lead to drastic declination in catalytic activity in ORR, but rather high value for active energy of enzyme denaturation also manifested this magnetic nano-particle based electrode with Lac with relative high endurance to surrounding temperature.

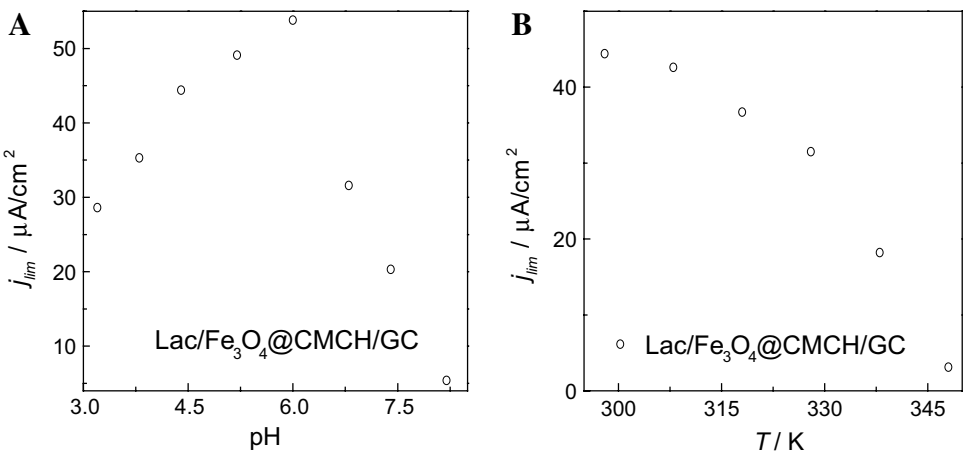

Fig. 11 Acid/base endurance (**a**) and thermal stability (**b**) of Lac/Fe_3O_4@CMCH/GC, test conditions as Fig. 8 demonstrated

Curves reflecting dependence of limited catalytic current density on consistency level of Cl^- dissolved in solution for two magnetic nano-particle based electrodes with Lac recorded in static state and in oxygen-bubbled PBS (temperature: 25 °C and pH of electrolyte was at 4.4) were displayed in Fig. 12, respectively. It was clear from Fig. 12 that catalytic current density was almost irrelevant to concentration of inhibitor: Cl^- for Lac/PHCTS-Fe_3O_4/GC and the influence of the inhibitor's presence on catalytic activity in ORR shouldn't be ignored for Lac/Fe_3O_4@CMCH/GC (catalytic performance in ORR would decrease drastically in the presence of Cl^-). This phenomenon should be correlated with interaction between enzyme carrier and immobilized enzyme molecules and electro-static interaction occurred between surface-tailored functional groups of matrix to entrap protein and halogen ion.

3.3 Quantitative Analysis on Kinetics of Enzymatic ORR Occurred on Two Lac-Based Electrodes Overlapped by Magnetic Nano-Particles with Different Chemical Composition

Rate determining step could be confirmed only if apparent rate constant of every step in the whole catalytic cycle for Lac-based electrodes was compared at the same dimension. Details for confirmation were illustrated as following:

a) for the case of efficient electron transfer in the presence of external mediator in terms of Lac/Fe_3O_4@CMCH/GC, the whole catalytic cycle was divided into several procedures (including mass transferring, charge transfer and chemical transformation) and rate constant of every step was evaluated as mentioned previously or as the method introduced in relevant literatures. Apparent diffusion rates for oxidized and reduced species of ABTS were determined to be 4.5 and 4.4×10^{-6} cm^2 s^{-1} [34], respectively. Accordingly normalized rate constants of diffusion in electrolyte for oxidized and reduced species of ABTS and dissolved di-oxygen molecules derived from normalization of mass transferring rate to active surface area of electrode were calculated to be 1.32, 1.29 and 5×10^{-5} s^{-1}, respectively. Standard reaction rate constant of Lac induced catalysis for chemical oxidation of $ABTS^{2-}$ occurred on the surface of Lac-based electrode was evaluated to be 0.033 s^{-1} according to the definition of specific activity for enzymatic catalysis and relevant spectrophotometry demonstrated in [33, 38]. Mean consuming rate of oxygen was measured by recording the relationship of oxygen consistency in aqueous solution and time elapsed with Clark oxygen electrode as depicted in [37] and the normalized rate constant for chemical adsorption of oxygen on the surface of electrode was derived from normalization of known consuming rate of oxygen dissolved in electrolyte to volume of solution and enzyme loading amount on the surface of Lac-based electrode referred in the previous section to be 0.097 s^{-1}. Moreover in combination with the fact that electro-chemical reduction rate constant of enzymatic oxidized species of ABTS occurred on the interface of electrode was estimated to be 23.0 s^{-1} as referred in the previous part of this article, the rate determining step in the whole catalysis should be ascribed to the diffusion process of mediator for Lac/Fe_3O_4@CMCH/GC. Thus the application of mediator with high mobility and stability can enhance the catalytic effect on ORR and promote the performance of this Lac-based electrode.

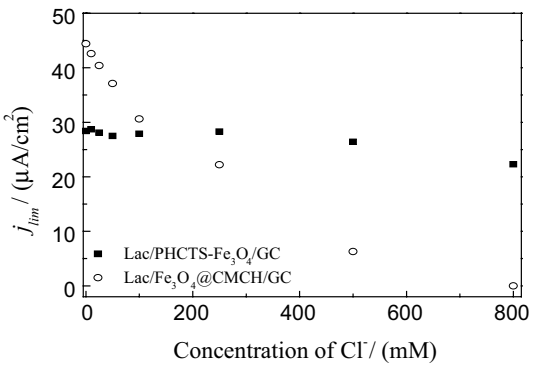

Fig. 12 Resistance to inhibitor Cl^- in catalytic performance of electrodes based on two kinds magnetic nano-particles with immobilized Lac, test conditions as Fig. 6 of [28] and Fig. 8 demonstrated, respectively

b) Following the same way, rate determining step in the catalytic cycle for Lac/PHCTS-Fe_3O_4/GC can be validated through comparison in rate constants of each step for the whole catalysis under the same dimension. In contrast to the case of Lac/Fe_3O_4@CMCH/GC, that of Lac/PHCTS-Fe_3O_4/GC didn't comprise the process of mediator diffusion and the enzyme-induced chemical transformation. Rate constant of intra-molecular electron transfer was high up to 10^3 s^{-1} only if the micro-environment of active site in Lac didn't vary substantially [33]. Acting as the same route depicted in the last paragragh, rate constant for chemical attachment of oxygen dissolved in solution on the binding site in Lac immobilized on the surface of electrode was measured to be 0.021 s^{-1}. Together with provided rate constant of oxygen diffusion into the over-coat layer with entrapped Lac (derived from the normalization of diffusion rate mentioned in Sect. 3.2.2 to active surface area, i.e. 2.1×10^{-7} s^{-1}), rate constant of direct electron transfer between electrode and redox protein (0.05 s^{-1}) and that of electrochemical transformation for ORR

($0.3\ s^{-1}$), it can be deduced from the analysis that key limiting factor in the whole catalysis of ORR for Lac/PHCTS-Fe_3O_4/GC should be attributed to the mass transferring process which was similar to the system discussed in [36]. Therefore the valid means to improve the performance of this electrode included the adjustment in porosity of nano-particles which allow oxygen to penetrate efficiently into the modification layer overcoated on the surface of electrode and modulation in capability to accommodate substrate and so on.

4 Conclusion

Efficient electron shuttle and catalysis for ORR can be achieved in the presence of external electron mediator for Lac/Fe_3O_4@CMCH/GC, while direct electron transfer between conductive matrix and T_1 site in Lac which should be classified into a typical surface confined quasi reversible process of single electron and favorable catalytic function on ORR can be realized without the help of electron relay for Lac/PHCTS-Fe_3O_4/GC. Results from experiments revealed the latter exhibited better performance in reproducibility, long-term usability, mechanical robusticity, endurance to inhibitor and thermal stability of catalytic effect on ORR than the former. However optimal pH for the former was near physiological pH which was distinct from the case for the latter (optimal pH was close to weak acid condition). Rate determining steps for both of Lac-based electrodes should be attributed to the process of mediator diffusion (Lac/Fe_3O_4@CMCH/GC) and that of mass transferring for substrate (Lac/PHCTS-Fe_3O_4/GC), respectively. Result also suggested the surface anchored aromatic ring structure played the key role in promoting the efficiency of direct electrochemistry between electrode and cofactor in Lac.

Acknowledgements This study was financially supported by the National Natural Science Foundation of China (No. 21363024, 31560249), Xin-Jiang autonomous region 2013 annual colleges and universities scientific research plan-Young teacher cultivation project (No. XJEDU2013S29), Science and Technology Innovation Funding Project of Graduate Students in Xinjiang Normal University (XSY201502009) and PH D scientific initiate funding project of Xin-Jiang normal university (No. XJNUBS1228).

Appendix

See Fig. 13.

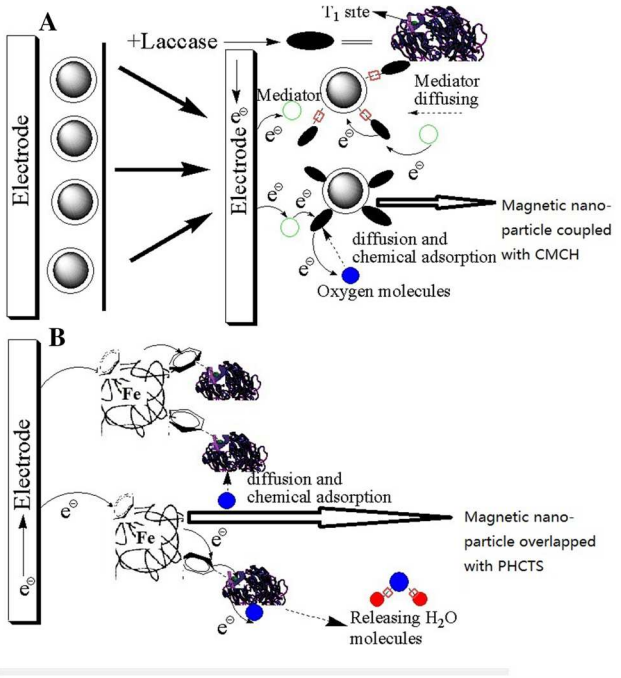

Fig. 13 Two kinds of Chitosan derivatives overlapped or coupled Fe_3O_4 magnetic nano-particles with immobilized Laccase molecules modified electrode showed different electron transfer mechanism between enzyme and conductive matrix

References

1. N. Lalaoui, R. David, H. Jamet, M. Holzinger, A.L. Goff, S. Cosnier, ACS. Catal. **6**, 4259 (2016)
2. C. Adam, P. Scodeller, M. Grattieri, M. Villalba, E.J. Calvo, Bioelectrochem. **109**, 101 (2016)
3. S.A. Neto, A.L.R.L. Zimbardi, F.P. Cardoso, L.B. Crepaldi, S.D. Minteer, J.A. Jorge, R.P.M. Furriel, A.R. De Andrade, J. Electroanal. Chem. **765**, 2 (2016)
4. H.Y. Zhao, H.M. Zhou, J.X. Zhang, W. Zheng, Y.F. Zheng. Biosens Bioelectron. **25**, 463 (2009)
5. M. Rasmussen, R.E. Ritzmann, I. Lee, A.J. Pollack, D. Scherson, J. Am. Chem. Soc. Bioelectron. **134**, 1458 (2012).
6. T. Chen, S.C. Barton, G. Binyamin, Z.Q. Gao, Y.C. Zhang, H.H. Kim, A. Heller, J Am Chem Soc. **123**, 8630 (2001)
7. C. Bunte, O. Prucker, T. Konig, J. Ruhe, Langmuir. **26**, 6019 (2010)
8. Y. Liu, M.K. Wang, F. Zhao, B.F. Liu, S.J. Dong, Chem. Eur. J. **11**, 4970 (2005)
9. M.T. Meredith, M. Minson, D. Hickey, K. Artyushkova, D.T. Glatzhofer, S.D. Minteer, ACS Catal. **1**, 1683 (2011)
10. C.D. Bari, A. Goni-Urtiaga, M. Pita, S. Shleev, M.D. Toscano, R. Sainz, A.L. De Lacey, Electrochim. Acta. **191**, 500 (2016)
11. L. Quintanar, J.J. Yoon, C.P. Aznar, A.E. Palmer, K.K. Andersson, R.D. Britt, E.I. Solomon, J. Am. Chem. Soc. **127**, 13832 (2005)
12. T. Kuwahara, K. Nakata, M. Kondo, M. Shimomura, Synthe. Mater. **214**, 30 (2016)
13. A.M. Wen, N.F. Steinmetz. Chem. Soc. Rev. **45**, 4074 (2016)
14. W. Nakanishi, K. Minami, L.K. Shrestha, Q.M. Ji, J.P. Hill, K. Ariga, Nano. Today. **9**, 378 (2014)

15. E.K. Lim, T. Kim, S. Paik, S. Haam, Y.M. Huh, K. Lee, Chem. Rev. **115**, 327 (2015)
16. K. Ariga, K. Minami, M. Ebara, J. Nakanishi, Polym. J. **48**, 371 (2016)
17. A. Bekhoukh, A. Zehhaf, A. Benyoucef, S. Bousalem, M. Belbachir, J. Inorg. Organomet. Polym. (2016). Doi:10.1007/s10904-016-0433-4
18. F. Chouli, A. Zehhaf, A. Benyoucef, Macromol. Res. **22**, 26 (2014)
19. F. Chouli, I. Radja, E. Morallon, A. Benyoucef, Polym. Compos. (2016). Doi:10.1002/pc.23837
20. F.Z. Dahou, M.A. Khaldi, A. Zehhaf, A. Benyoucef, M.I. Ferrahi, Adv. In Polym. Technol. **35**, 411 (2016)
21. I. Radja, H. Djelad, E. Morallon, A. Benyoucef, Synthe. Mater. **202**, 25 (2015)
22. D.P. Tang, R. Yuan, Y.Q. Chai, J. Phys. Chem. B. **110**, 11640 (2006)
23. J.D. Qiu, H.P. Peng, R.P. Liang, Electrochem. Commun. **9**, 2734 (2007)
24. R. Nakamura, K. Kamiya, K. Hashimoto, Chem. Phys. Lett. **498**, 307 (2010)
25. D. Singh, K.K. Sharma, M.S. Dhar, J.S. Virdi, Biochem. Biophys. Res. Commun. **449**, 157 (2014)
26. N. Mano, L. Edembe, Biosens. Bioelectron. **50**, 478 (2013)
27. L.R. Yang, C. Guo, S. Chen, F. Wang, J. Wang, Z.T. An, C.Z. Liu, H.Z. Liu, Ind. Eng. Chem. Res. **48**, 944 (2009)
28. H. Zeng, Y. Yang, X.J. Li, X. Bai, Chin. J. Anal. Chem. **43**, 1794 (2015) (**in Chinese**)
29. J. Huang, J.Y. Zhou, H.Y. Xiao, S.Y. Long, J.T. Wang, Acta Chim. Sin. **63**, 1343 (2005) (**in Chinese**)
30. H. Zeng, S.X. Zhao, L.X. Gong, Z. Su, Chin. J. Appl. Chem. **30**, 436 (2013) (**in Chinese**)
31. Y. Yang, H. Zeng, Q. Zhang, X. Bai, C. Liu, Y.H. Zhang, Chem. Phys. Lett. **658**, 259 (2016)
32. A.E. Palmer, S.K. Lee, E.I. Solomon, J. Am. Chem. Soc. **123**, 6591 (2001)
33. H.J. Qiu, C.X. Xu, X.R. Huang, Y. Ding, Y.B. Qu, P.J. Gao, J. Phys. Chem. C. **112**, 14781 (2008)
34. H. Zeng, Z.Q. Tang, L.W. Liao, J. Kang, Y.X. Chen, Chin. J. Chem. Phys. **24**, 653 (2011)
35. N. Mano, H.H. Kim, Y.C. Zhang, A. Heller, J. Am. Chem. Soc. **124**, 6480 (2002)
36. S. Tsujimura, Y. Kamitaka, K. Kano, Fuel Cells **7**, 463 (20070
37. W.E. Farneth, M.B. D'Amore, J. Electroanal. Chem. **581**,197 (2005)
38. H.J. Qiu, C.X. Xu, X.R. Huang, Y. Ding, Y.B. Qu, P.J. Gao, J. Phys. Chem. C. **113**, 2521 (2009)